

Core level binding energies in solids from first-principles

- Introduction of XPS
- Absolute binding energies of core states
- Applications to silicone
- Outlook

TO and C.-C. Lee, Phys. Rev. Lett. 118, 026401 (2017).

C.-C. Lee et al., Phys. Rev. B 95, 115437 (2017).

Taisuke Ozaki (ISSP, Univ. of Tokyo)

The Winter School on DFT: Theories and Practical Aspects, Dec. 19-23, CAS.

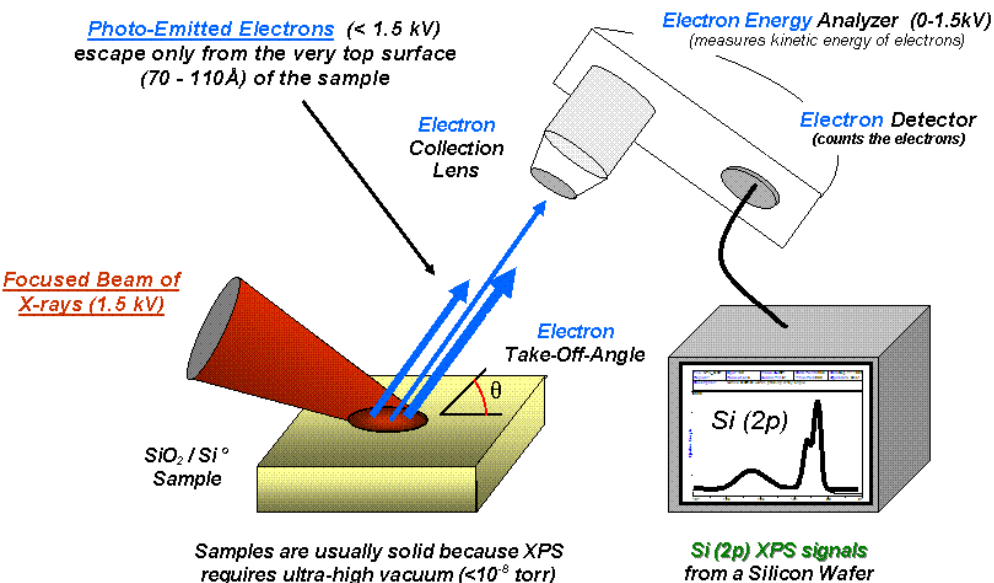
X-ray photoemission spectroscopy(XPS)

- Information of chemical composition, surface structure, surface absorbate
- XPS with synchrotron radiation extends its usefulness, e.g., satellite analysis, core level vibrational fine structure, XPS circular dichroism, spin-resolved XPS, and XPS holography.

We have developed a general method to calculate absolute binding energies of core levels in solids with the following features:

- applicable to **insulators** and metals
- accessible to **absolute** binding energies
- screening of core and valence electrons on the same footing
- SCF treatment of spin-orbit coupling
- exchange interaction between core and valence states
- geometry optimization with a core hole state

XPS experiments

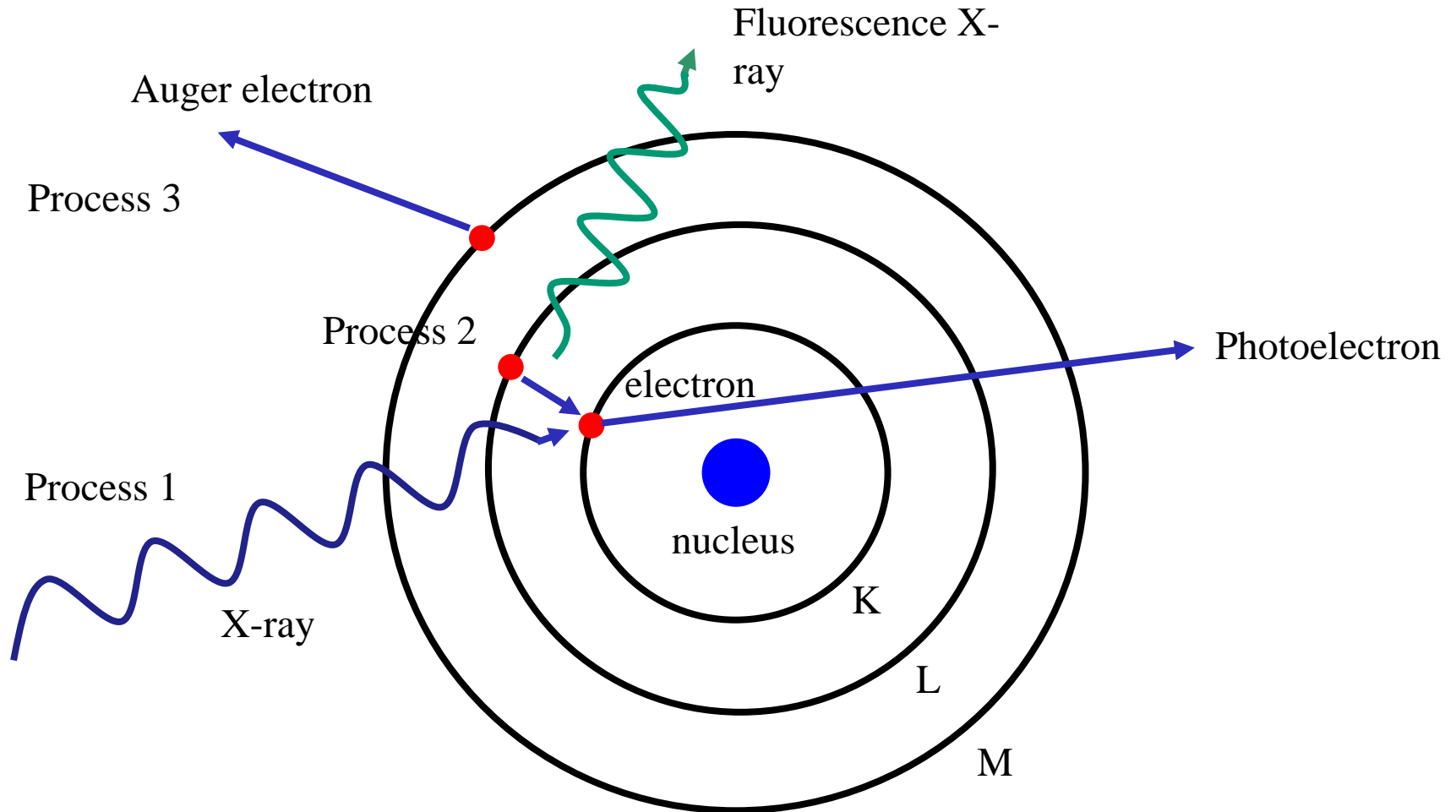


Appearance of XPS equipment



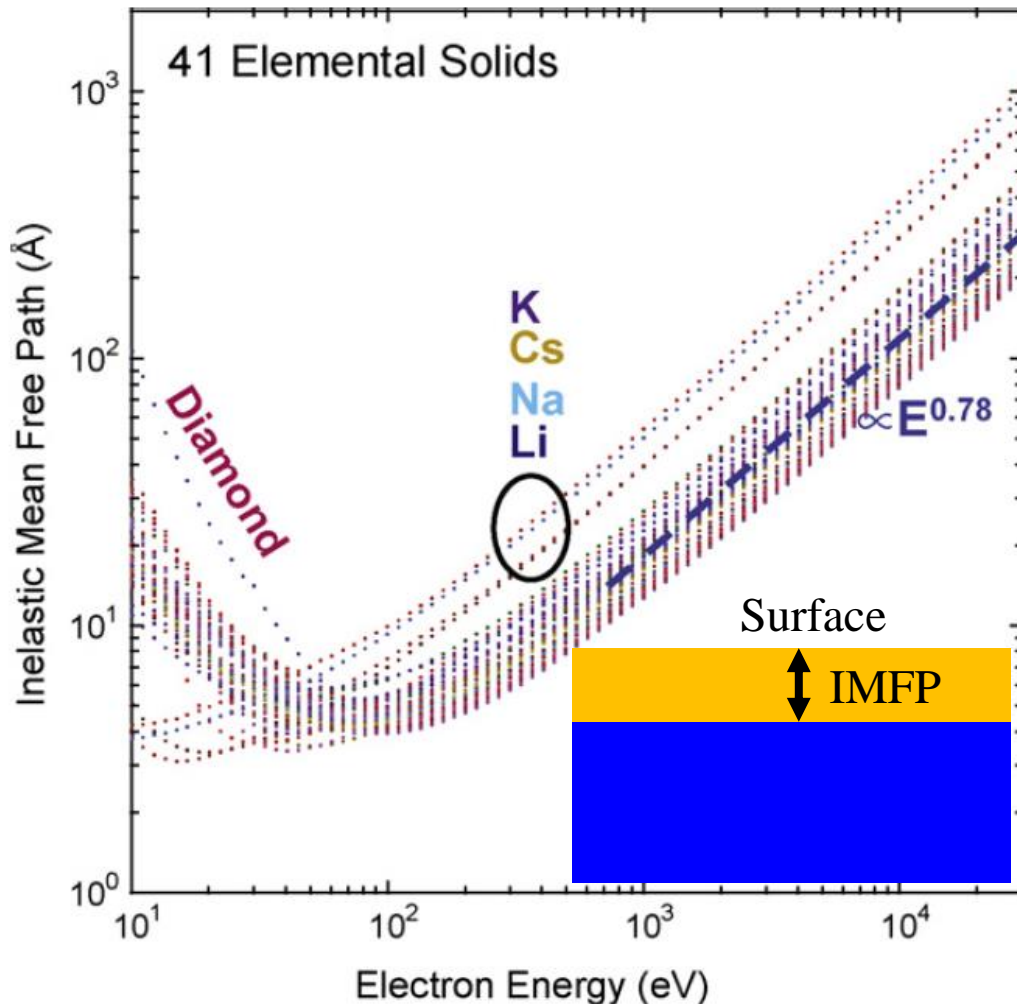
In general, XPS requires high vacuum ($P \sim 10^{-8}$ millibar) or ultra-high vacuum (UHV; $P < 10^{-9}$ millibar) conditions.

Basic physics in X-ray photoelectron spectroscopy (XPS)



Escape time of photoelectron seems to be considered around 10^{-16} sec., resulting in relaxation of atomic structure would be ignored.

Surface sensitivity

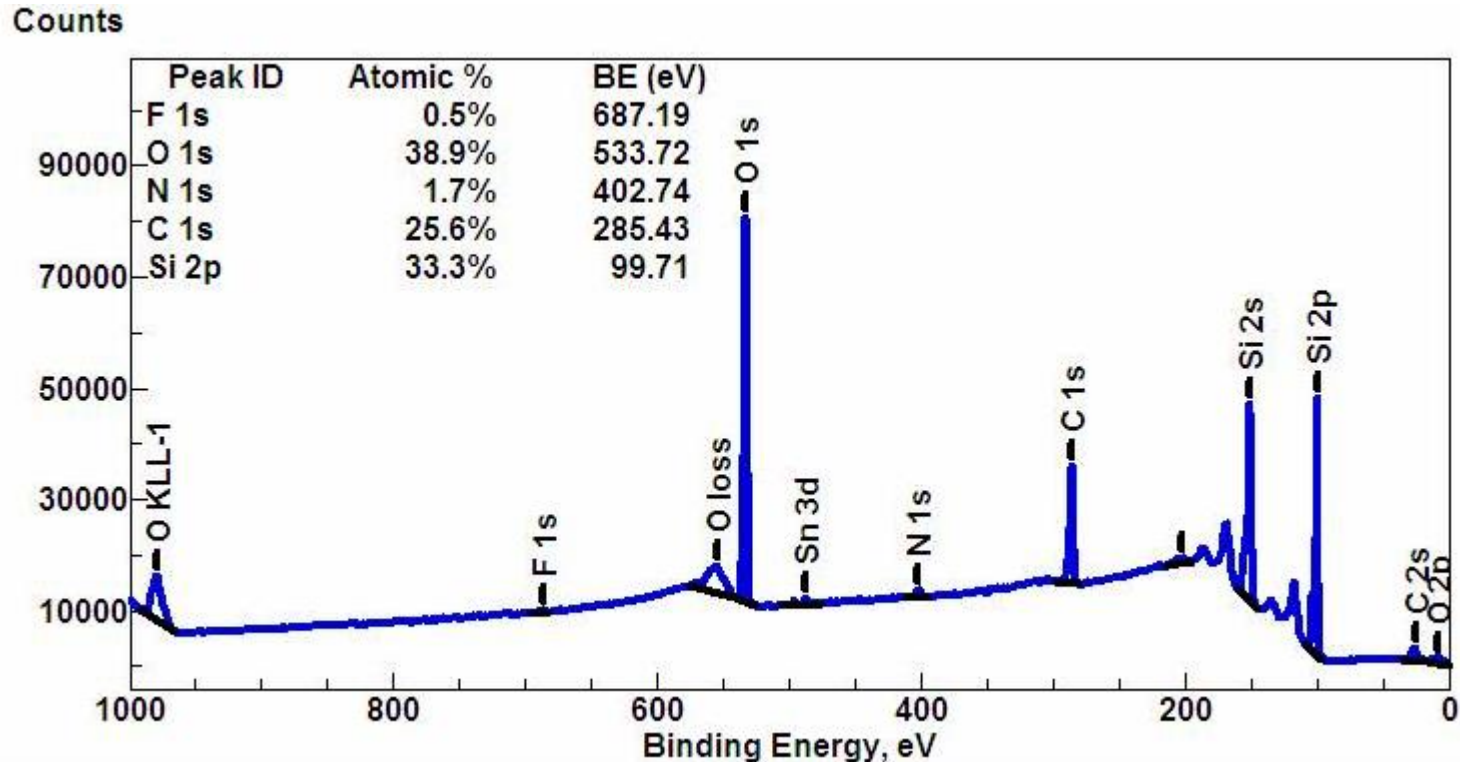


C.S. Fadley, Journal of Electron Spectroscopy and Related Phenomena 178-179, 2 (2010).

Fig. 2. Inelastic mean free paths (IMFPs) for 41 elements, calculated using the TPP-2M formula: Li, Be, three forms of carbon (graphite, diamond, glassy C), Na, Mg, Al, Si, K, Sc, Ti, V, Cr, Fe, Co, Ni, Cu, Ge, Y, Nb, Mo, Ru, Rh, Pd, Ag, In, Sn, Cs, Gd, Tb, Dy, Hf, Ta, W, Re, Os, Ir, Pt, Au, and Bi. Five “outlier” elements are indicated to provide some idea of what electronic structure characteristics can give rise to deviations from the majority behavior: diamond and the alkali metals. The dashed straight line for higher energies represents a variation as $\Lambda_e \propto E_{kin}^{0.78}$, and is a reasonable first approximation to the variation for all of the elements shown (from Ref. [23]).

- Inelastic Mean Free Path (IMFP) of photo excited electron for 41 elemental solids is shown the left figure.
- In case of the widely used aluminum K-alpha X-ray having 1486.7 eV, the IMFP is found to be 15 ~ 100 Å.
- On the other hand, when X-rays generated by synchrotron radiation is utilized, which have energy up to 15 keV, the IMFP can be more than 100 Å.

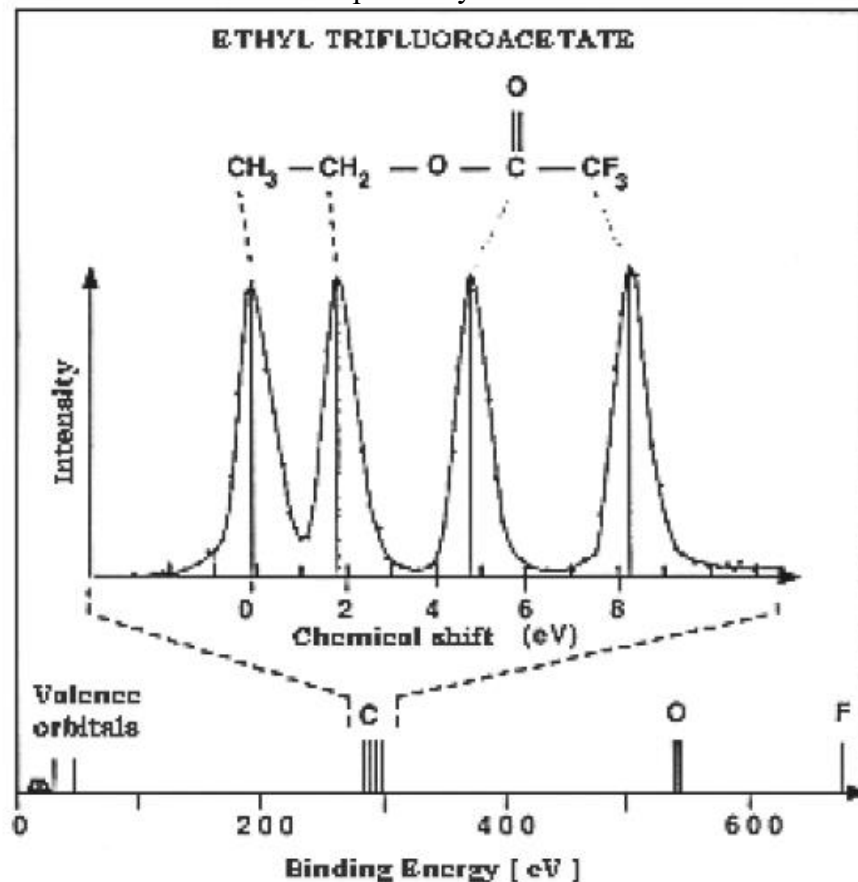
Element specific measurement



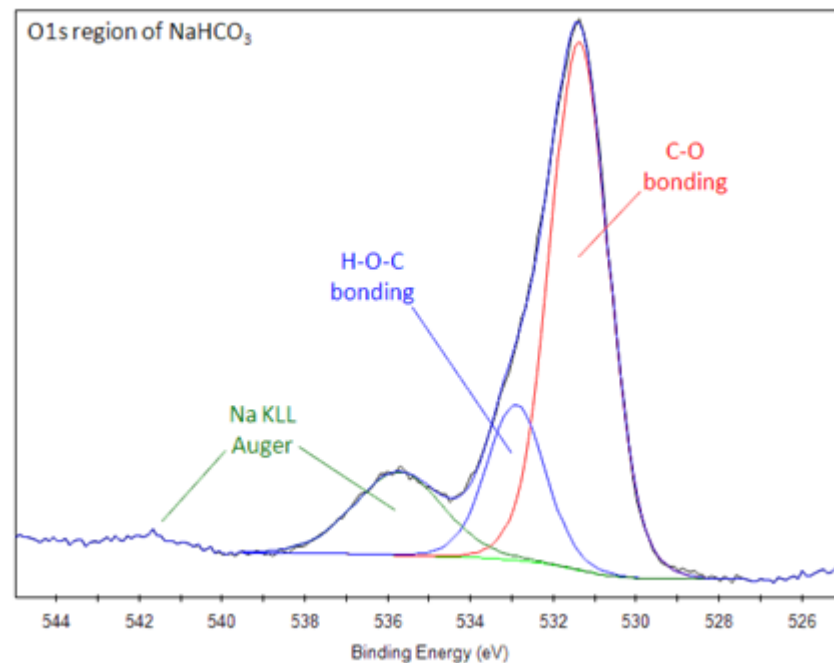
- The binding energy of each core level in each element is specific, and by this reason one can identify element and composition in a material under investigation by a wide scan mode, while hydrogen and helium cannot be identified because of low binding energies overlapping to other valence states.
- The database which is a huge collection of experimental data measured by XPS is available at <http://srdata.nist.gov/xps/Default.aspx>

Sensitivity to chemical environment

“PHOTOEMISSION SPECTROSCOPY
Fundamental Aspects” by Giovanni Stefani



H. Nohira et al., Journal of Non-Crystalline Solids 303 (2002) 83–87



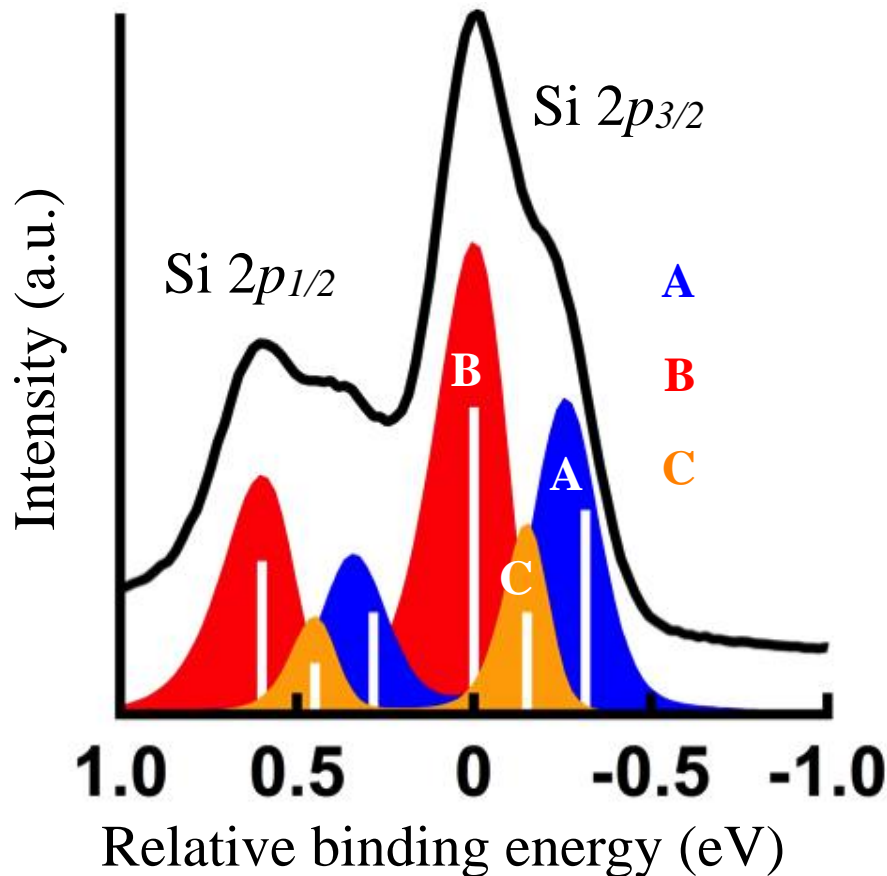
- The binding energy shifts depending on its chemical environment. The amount of shift is primarily determined by its charge state, known to be **initial state effect**.
- After creating the core hole, the screening of the core hole is also an important factor to determine chemical shift, known to be **final state effect**.

Core level multiplet splittings: Spin-orbit splitting

In addition to the chemical shift, there are other multiplet splittings.

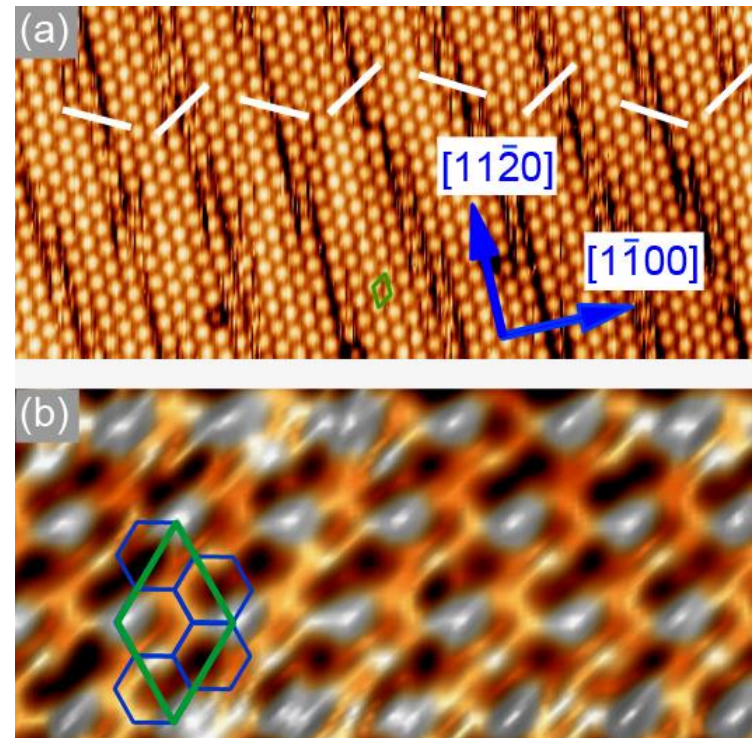
Spin-orbit coupling of core level

- Due to the strong SOC of core level states, the binding energy is split into two levels.
- The intensity ratio is $2l: 2(l+1)$ for $l-1/2$ and $l+1/2$, respectively.



A. Fleurence et al., PRL 108, 245501 (2012).

Silicene on ZrB₂ surface



Core level multiplet splittings: Exchange interaction

Exchange interaction between core and valence electrons

- After creation of core hole, the remaining core electron is spin polarized.
- If the valence electron is spin polarized in the initial state, there must be an exchange interaction between the remaining core electron and valence electrons even in the final state.
- The exchange interaction results in multiplet splitting.
- The left figure (A) shows that the 1s binding energy of oxygen and nitrogen atom splits in magnetic molecules O_2 and NO , respectively, while no splitting is observed in N_2 being a non-magnetic molecule.
- The right figure (B) shows the splitting of 3s binding energy of Mn atom in manganese compounds.

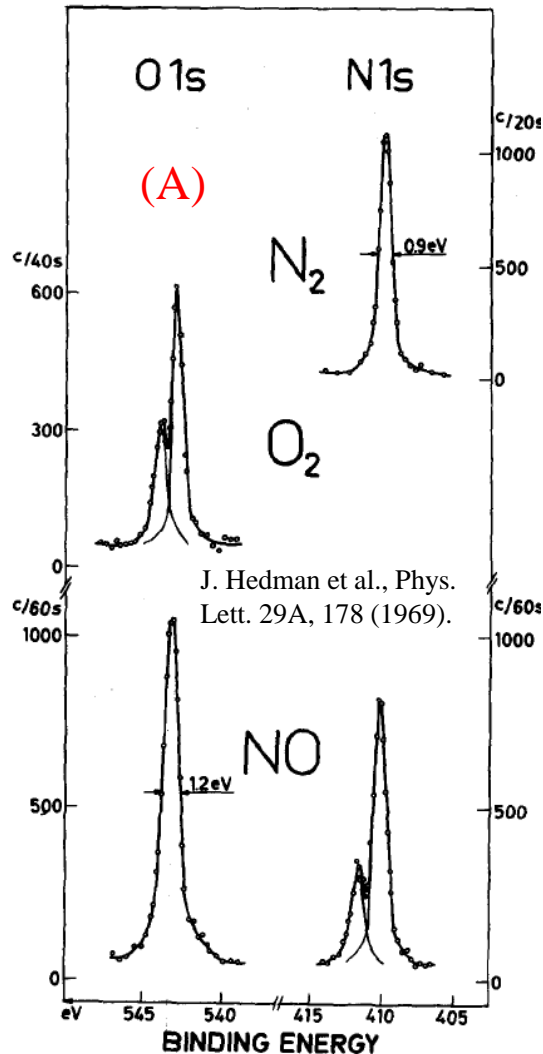


Fig. 1. ESCA spectra of core electron levels in N_2 , O_2 , and NO . Paramagnetic splitting is observed for the 1s levels in the O_2 and NO molecules.

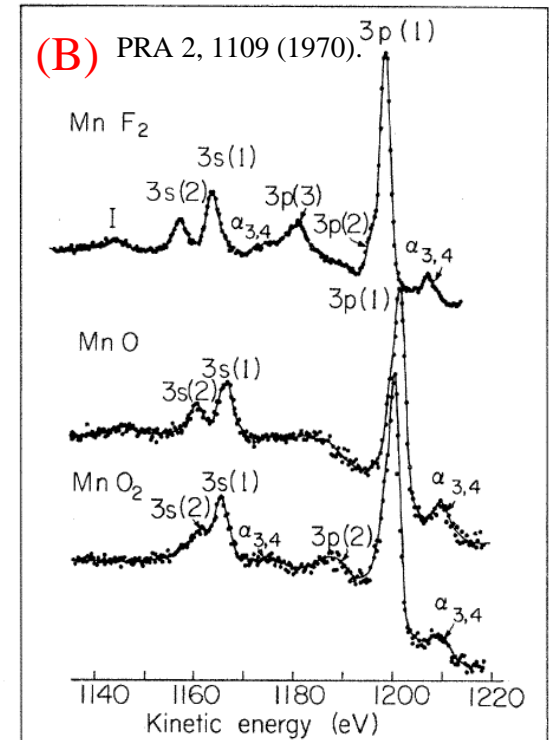
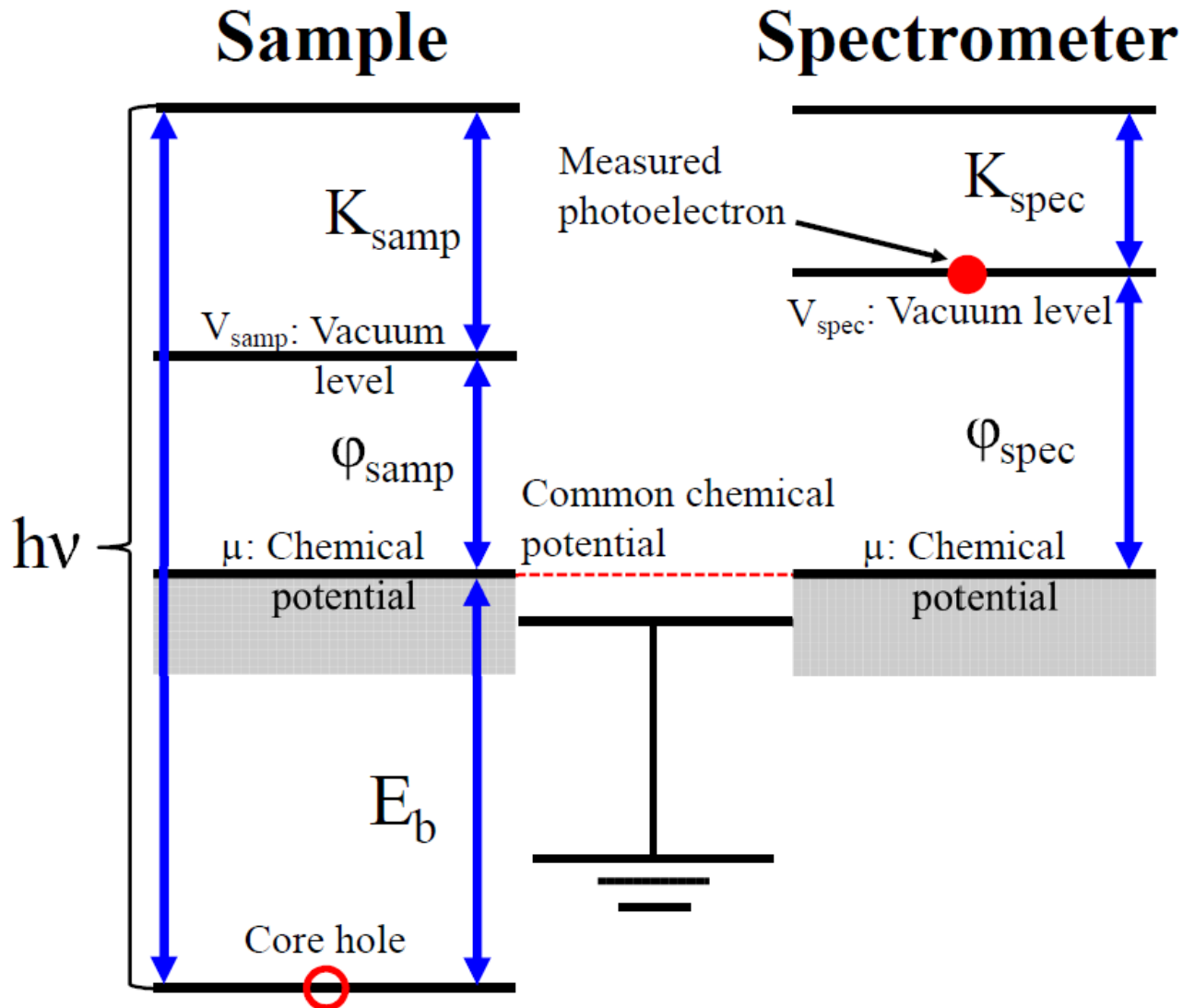


FIG. 1. Photoelectron spectra from MnF_2 , MnO , and MnO_2 in the kinetic-energy region corresponding to ejection of Mn 3s and 3p electrons by $Mg K\alpha$ x rays.

Energy conservation in XPS

$$E_i(N) + h\nu = E_f(N-1) + V_{\text{spec}} + K_{\text{spec}}$$



Core level binding energies in XPS #1

$$E_i(N) + h\nu = E_f(N-1) + V_{\text{spec}} + K_{\text{spec}}$$

Using a relation: $V_{\text{spec}} = \mu + \phi_{\text{spec}}$ we have

$$E_b = h\nu - K_{\text{spec}} - \phi_{\text{spec}} = E_f(N-1) - E_i(N) + \mu$$

The experimental chemical potential can be transformed as

$$E_b = E_f^{(0)}(N-1) + (N-1)\Delta\mu - (E_i^{(0)}(N) + N\Delta\mu) + \mu_0 + \Delta\mu$$

A general formula of core level binding is given by

$$E_b = E_f^{(0)}(N-1) - E_i^{(0)}(N) + \mu_0$$

This is common for metals and insulators.

Core level binding energies in XPS #2

For metals, the Janak's theorem simplifies the formula:

$$E_{\text{f}}^{(0)}(N-1) - E_{\text{f}}^{(0)}(N) = \int dn \partial E_{\text{f}}^{(0)} / \partial n = -\mu_0$$

$$E_{\text{b}} = E_{\text{f}}^{(0)}(N) - E_{\text{i}}^{(0)}(N)$$

The formulae of core level binding energies are summarized as

Solids (gapped
systems, metals)

$$E_{\text{b}} = E_{\text{f}}^{(0)}(N-1) - E_{\text{i}}^{(0)}(N) + \mu_0$$

Metals

$$E_{\text{b}} = E_{\text{f}}^{(0)}(N) - E_{\text{i}}^{(0)}(N)$$

Gases

$$E_{\text{b}} = E_{\text{f}}^{(0)}(N-1) - E_{\text{i}}^{(0)}(N)$$

Calculations: core level binding energy

Within DFT, there are at least three ways to calculate the binding energy of a core state as summarized below:

1. Initial state theory

Simply the density of states is taken into account

2. Core-hole pseudopotential method

Full initial and semi-final state effects are taken into account

E. Pehlke and M. Scheffler, PRL 71 2338 (1993).

3. Core-hole SCF method

The initial and final state effects are fully taken into account on the same footing.

The method 3 can be regarded as the most accurate scheme among the three methods, and enables us to obtain the absolute value of binding energy and splitting due to spin-orbit coupling and spin interaction between the remaining core state and spin-polarized valence states.

Constraint DFT with a penalty functional

$$E_f = E_{\text{DFT}} + E_p$$

E_{DFT} is a conventional functional of DFT, and E_p is a penalty functional defined by

$$E_p = \frac{1}{V_B} \int dk^3 \sum_{\mu} f_{\mu}^{(\mathbf{k})} \langle \psi_{\mu}^{(\mathbf{k})} | \hat{P} | \psi_{\mu}^{(\mathbf{k})} \rangle$$

$$\hat{P} = \left| R\Phi_J^M \right\rangle \Delta \left\langle R\Phi_J^M \right| \quad \text{R: radial function of the core level}$$

The projector is given by a solution of Dirac eq. for atoms.

$$\begin{aligned} J = l + \frac{1}{2}, M = m + \frac{1}{2} & \quad J = l - \frac{1}{2}, M = m - \frac{1}{2} \\ |\Phi_J^M\rangle = \left(\frac{l+m+1}{2l+1}\right)^{\frac{1}{2}} |Y_l^m\rangle + \left(\frac{l-m}{2l+1}\right)^{\frac{1}{2}} |Y_l^{m+1}\rangle & \quad |\Phi_J^M\rangle = \left(\frac{l-m+1}{2l+1}\right)^{\frac{1}{2}} |Y_l^{m-1}\rangle + \left(\frac{l+m}{2l+1}\right)^{\frac{1}{2}} |Y_l^m\rangle \end{aligned}$$

Kohn-Sham eq. with a penalty operator

By variationally differentiating the penalty functional E_f , we obtain the following the KS equation.

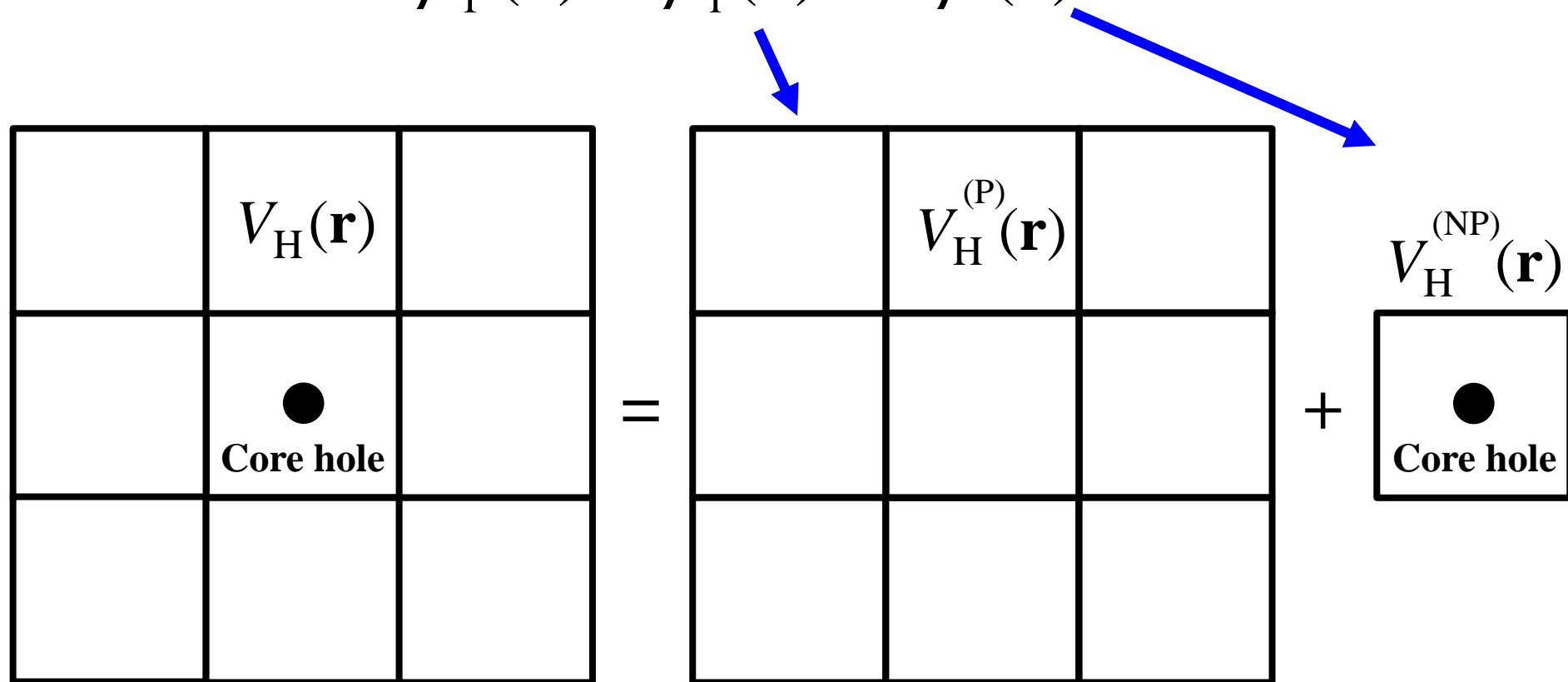
$$\left(\hat{T} + V_{\text{eff}} + \hat{P} \right) | \psi_{\mu}^{(\mathbf{k})} \rangle = \varepsilon_{\mu}^{(\mathbf{k})} | \psi_{\mu}^{(\mathbf{k})} \rangle$$

Features of the method

- applicable to insulators and metals
- accessible to absolute binding energies
- screening of core and valence electrons on the same footing
- SCF treatment of spin-orbit coupling
- exchange interaction between core and valence states
- geometry optimization with a core hole state

Elimination of inter-core hole interaction

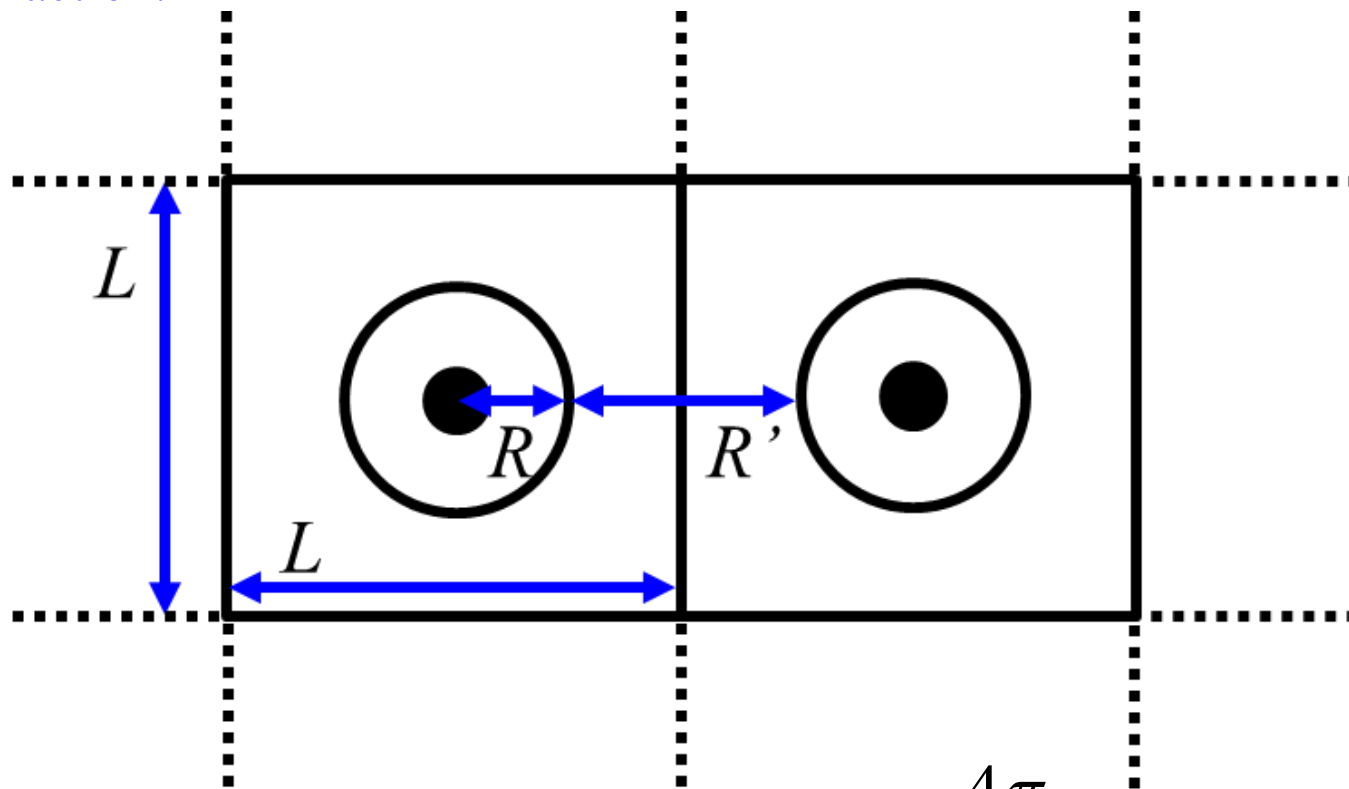
$$\rho_f(\mathbf{r}) = \rho_i(\mathbf{r}) + \Delta\rho(\mathbf{r}) \quad \Delta\rho(\mathbf{r}) = \rho_f(\mathbf{r}) - \rho_i(\mathbf{r})$$



- Periodic Hartree potential is calculated by charge density of the initial state.
- Potential by induced charge is calculated by an exact Coulomb cutoff method.

Exact Coulomb cutoff method #1

If the charge induced by a core hole localizes within a radius of R , we can set $R_c = 2R$, and the cutoff condition becomes $2R_c < L$ to eliminate the inter-core hole interaction.



$$v_H(r) = \sum_{\mathbf{G}} \frac{v(\mathbf{G})}{G} e^{i\mathbf{G} \cdot \mathbf{r}} \quad v(\mathbf{G}) = \frac{4\pi}{G^2} (1 - \cos GR_c)$$

Exact Coulomb cutoff #2

$$v_H(r) = \int dr' n(r') v(|r - r'|) \quad \dots(1)$$

$$n(r) = \sum_{\mathbf{G}} n(\mathbf{G}) e^{i\mathbf{G} \cdot \mathbf{r}} \quad \dots(2) \quad v(r) = \sum_{\mathbf{G}} v(\mathbf{G}) e^{i\mathbf{G} \cdot \mathbf{r}} \quad \dots(3)$$

By inserting (2) and (3) into (1), and performing the integration, we obtain

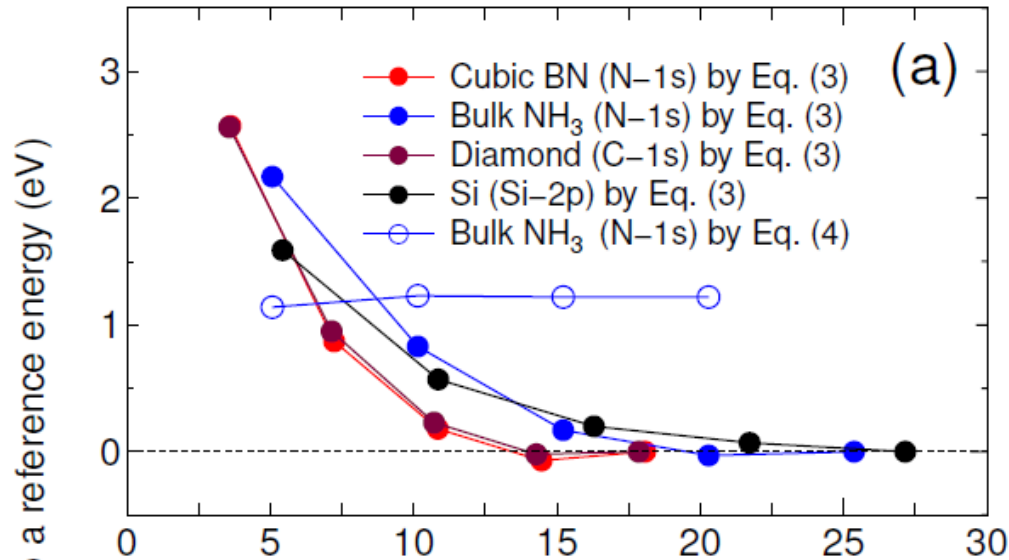
$$v_H(r) = \sum_{\mathbf{G}} n(\mathbf{G}) v(\mathbf{G}) e^{i\mathbf{G} \cdot \mathbf{r}}$$

$v(\mathbf{G})$ is evaluated by performing the integration as

$$v(r) = \frac{1}{r} \quad \text{if } r \leq R_c \quad v(\mathbf{G}) = \int_0^{R_c} dr r^2 \int_0^{2\pi} d\phi \int_0^\pi d\theta \sin \theta \frac{e^{i\mathbf{G} \cdot \mathbf{r}}}{r}$$

$$v(r) = 0 \quad \text{if } R_c < r \quad v(\mathbf{G}) = \frac{4\pi}{G^2} (1 - \cos GR_c)$$

Convergence w. r. t cell size

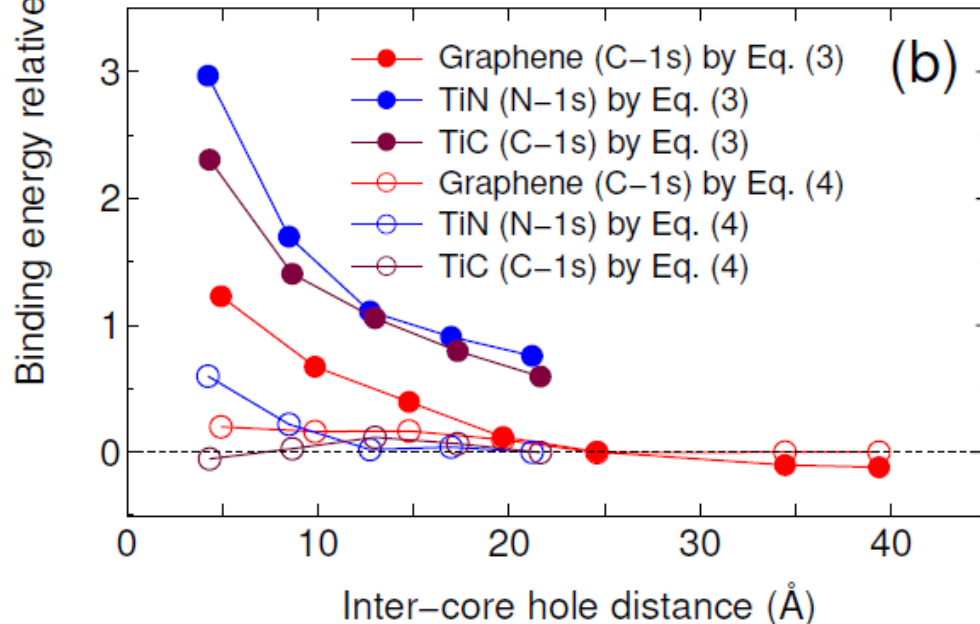


General formula

$$E_b = E_f^{(0)}(N-1) - E_i^{(0)}(N) + \mu_0 \quad \dots(3)$$

For metals

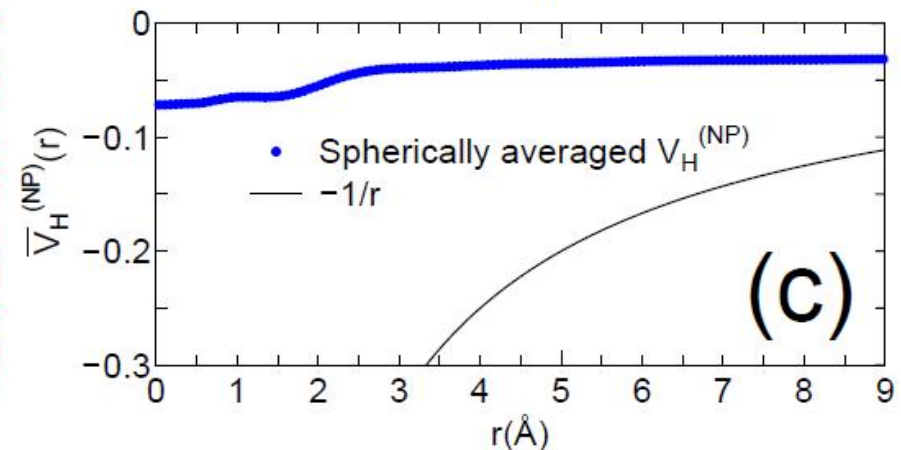
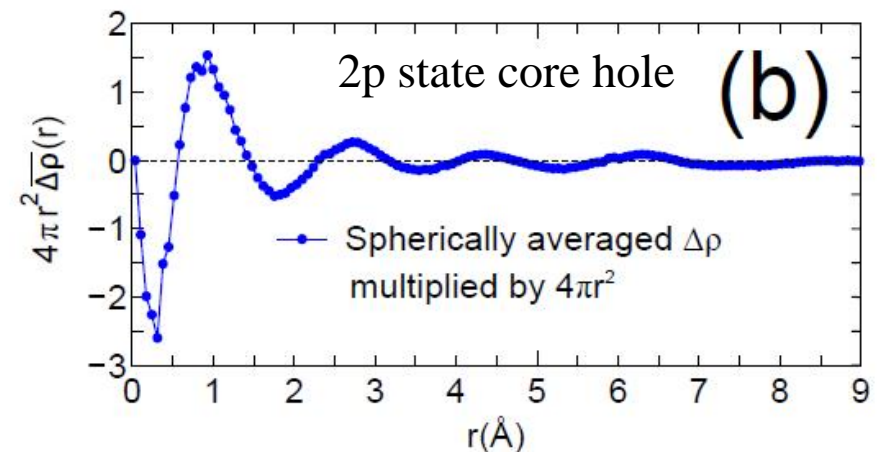
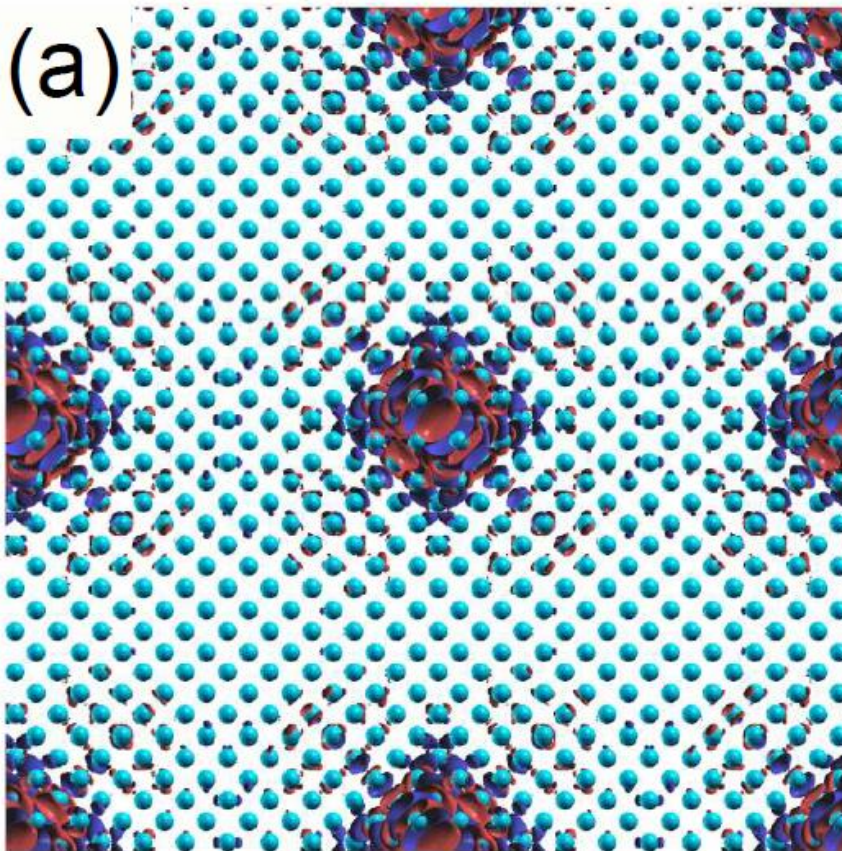
$$E_b = E_f^{(0)}(N) - E_i^{(0)}(N) \quad \dots(4)$$



- Convergence is attainable around 15~20Å.
- The formula for metals is not applicable for gapped systems.
- Very fast convergence by Eq. (4) for metals.

Difference charge induced by a core hole in Si

- The effective radius is about 7Å.
- The core hole is almost screened on the same Si atom.



Absolute values: Expt. vs. Calcs. for **solids**

Material	State	Calc. (eV)	Expt. (eV)
<i>Gapped system</i>			
c-BN	N-1s	398.87	398.1*
bulk NH ₃	N-1s	398.92	399.0 ⁺
Diamond	C-1s	286.50	285.6 [†]
Si	Si-2p _{1/2}	100.13	99.8*
Si	Si-2p _{3/2}	99.40	99.2*
<i>Semimetal or Metal</i>			
Graphene	C-1s	284.23	284.4 [†]
TiN	N-1s	396.43	397.1 [§]
TiC	C-1s	281.43	281.5*

Mean absolute error: 0.4 eV, Mean relative error: 0.16 %

Absolute values: Expt. vs. Calcs. for **gases**

Molecule	Calc. (eV)	Expt.* (eV)
<i>C-1s state</i>		
CO	295.87	296.19
C ₂ H ₂	291.24	291.17
CO ₂	296.89	297.66
HCN	293.35	293.50
C ₂ H ₄	290.50	290.79
H ₂ CO	294.00	294.47
<i>N-1s state</i>		
N ₂	409.89	409.83
NH ₃	404.70	405.60
N ₂ H ₄	404.82	406.1
HCN	406.16	406.36
<u>N</u> NO	408.24	408.66
<u>N</u> NO	411.98	412.57
NO(S=0)	410.62	411.6
NO(S=1)	410.10	410.2

Molecule	Calc. (eV)	Expt.* (eV)
<i>O-1s state</i>		
CO	542.50	542.4
CO ₂	541.08	541.2
O ₂ (S= $\frac{1}{2}$)	543.15	544.2
O ₂ (S= $\frac{3}{2}$)	542.64	543.1
H ₂ O	539.18	539.9
<i>Si-2p state</i>		
SiH ₄	106.56	107.3
Si ₂ H ₆	106.21	106.86
SiF ₄	111.02	111.7
SiCl ₄	109.32	110.2

Mean absolute error: 0.5 eV

Mean relative error: 0.22 %

Characterization of silicene structure

PRL 108, 245501 (2012).

PRB 90, 075422 (2014).

PRB 90, 241402 (2014).

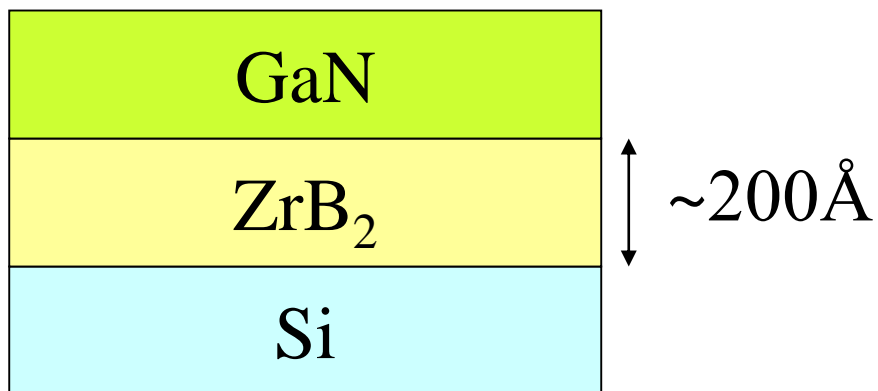
arXiv:1610.03131.

Experimental report of silicene on $\text{ZrB}_2(0001)$

Yamada-Takamura group of JAIST

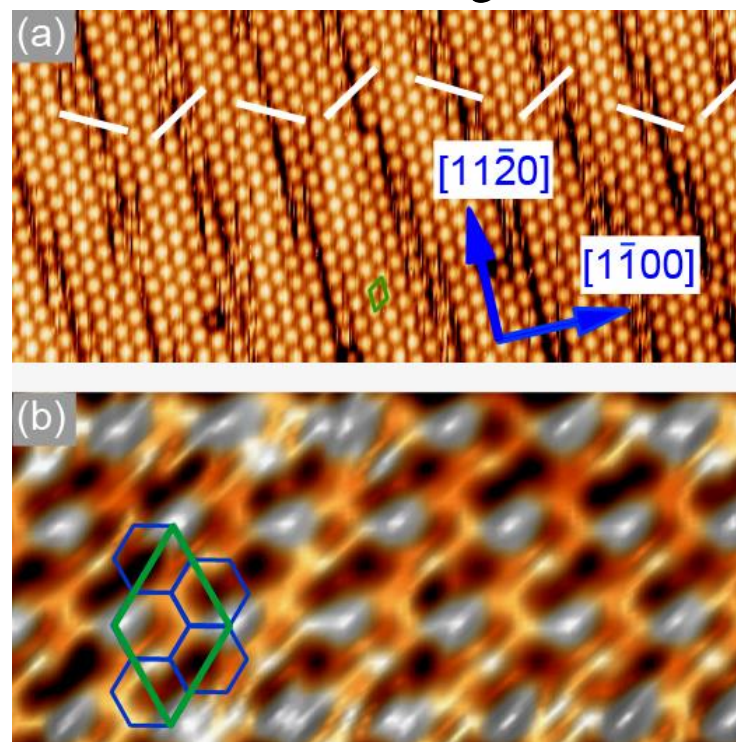
ZrB_2 on Si(111) is a promising substrate for a photo emitting device of GaN due to the lattice matching, metallicity, and flatness. It was found that Si atoms form a super structure during CVD by probably migration and segregation of Si atoms from the Si substrate.

STM image



GaN(0001): $a = 3.189\text{\AA}$

$\text{ZrB}_2(0001)$: $a = 3.187\text{\AA}$

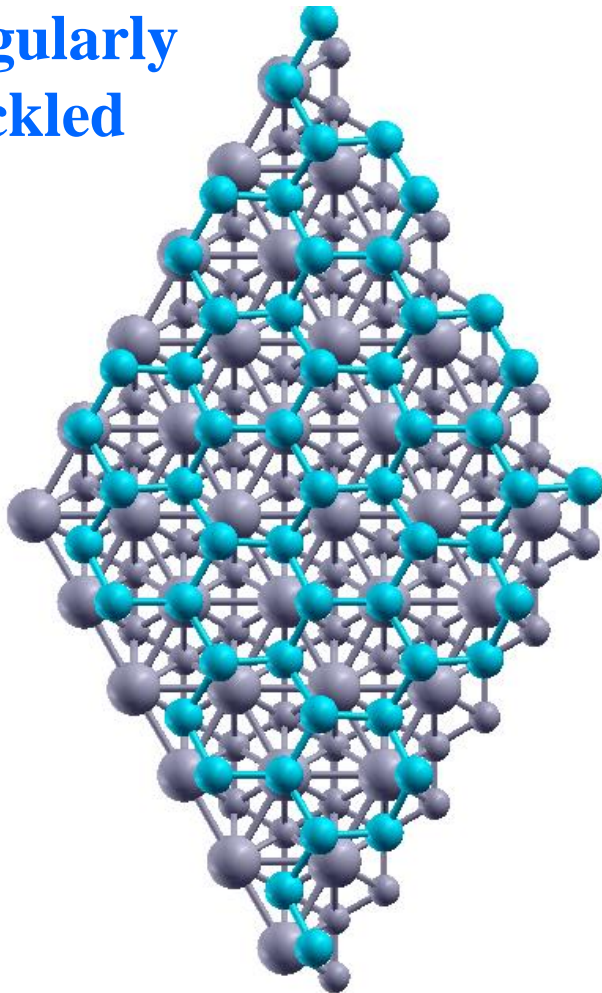


A. Fleurence et al., PRL 108, 245501 (2012).

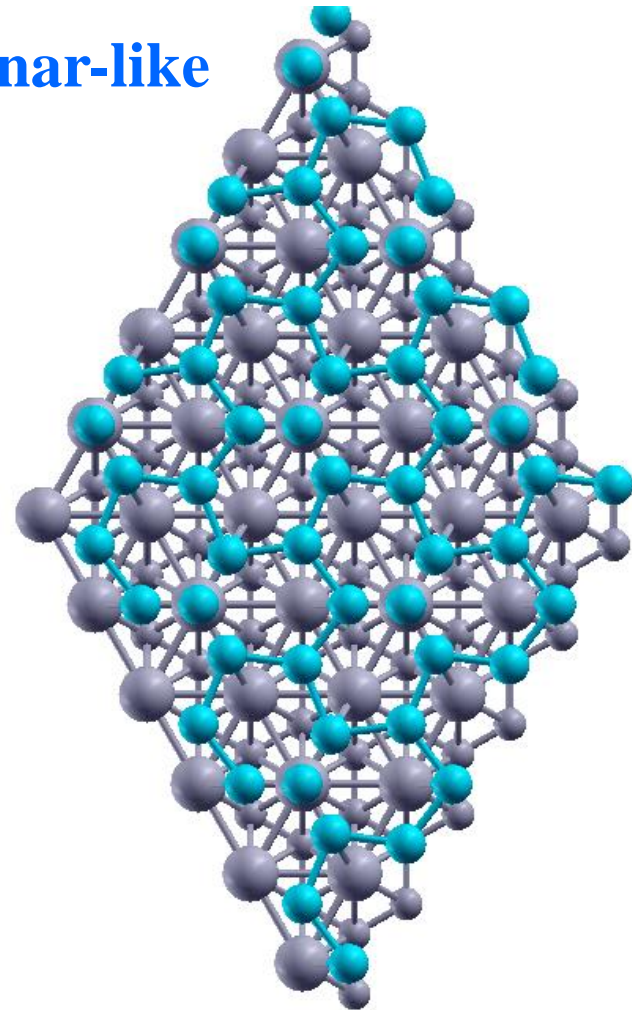
Top view of optimized structures

- Two buckled structures are obtained.
- Both the structures keep the honeycomb lattice.

**Regularly
buckled**



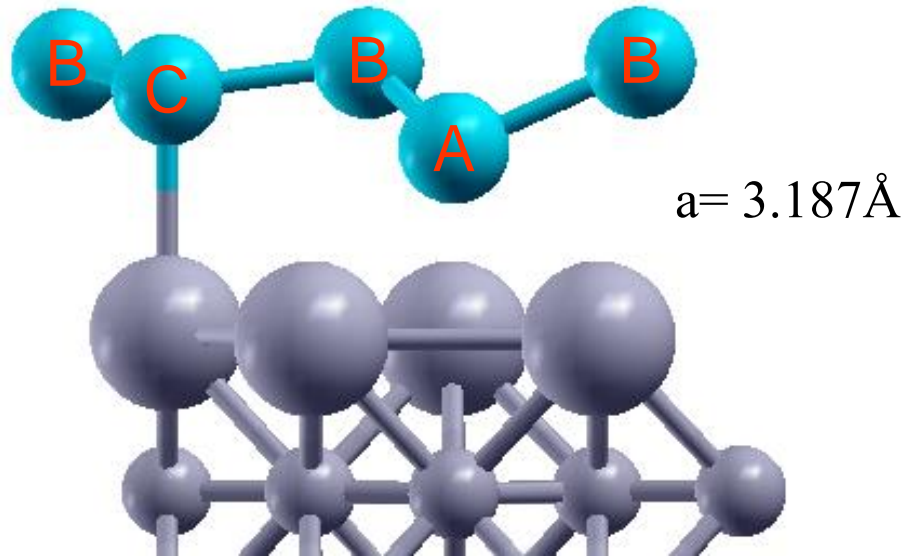
Planar-like



Optimized structures

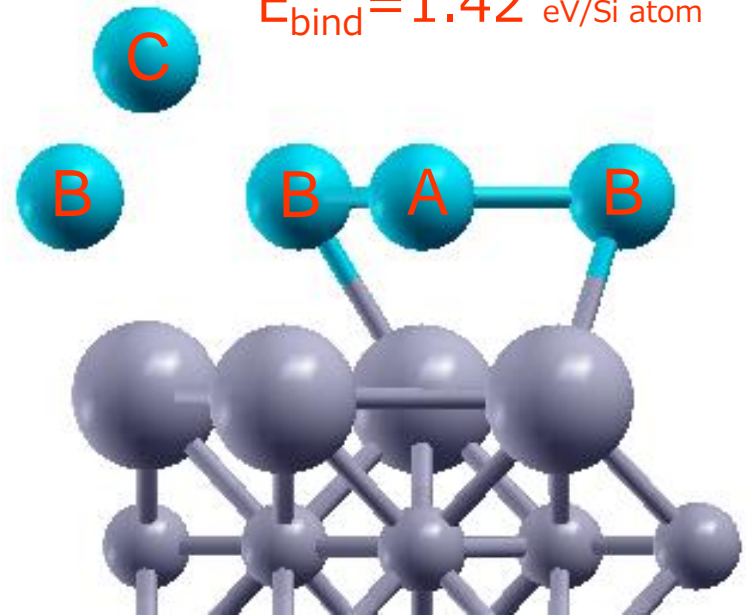
Regularly buckled

$$E_{\text{bind}} = 1.14 \text{ eV/Si atom}$$



Planar-like

$$E_{\text{bind}} = 1.42 \text{ eV/Si atom}$$



A B C

Distance from
the top Zr layer
(Ang.)

	A	B	C
Distance from the top Zr layer (Ang.)	2.105	3.043	2.749
Distance with neighbor Si atoms (Ang.)	2.263	2.268	2.249
Angle with neighbor Si atoms (Deg.)	104.2	110.1	118.2

Distance with
neighbor Si
atoms (Ang.)

Angle with
neighbor Si
atoms (Deg.)

A B C

	A	B	C
Distance from the top Zr layer (Ang.)	2.328	2.331	3.911
Distance with neighbor Si atoms (Ang.)	2.324	2.340	2.380
Angle with neighbor Si atoms (Deg.)	120.2	113.0	80.5

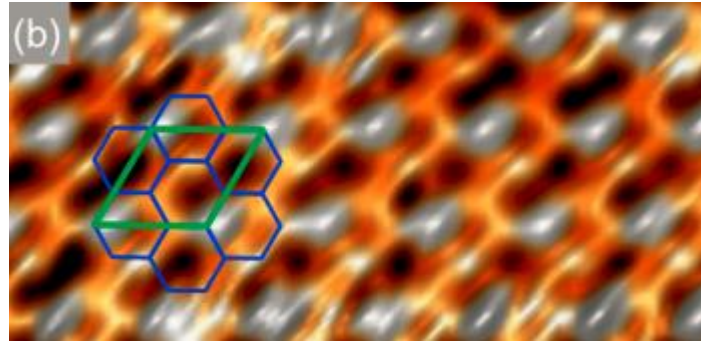
Distance with
neighbor Si
atoms (Ang.)

Angle with
neighbor Si
atoms (Deg.)

STM image

Expt.

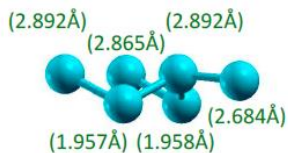
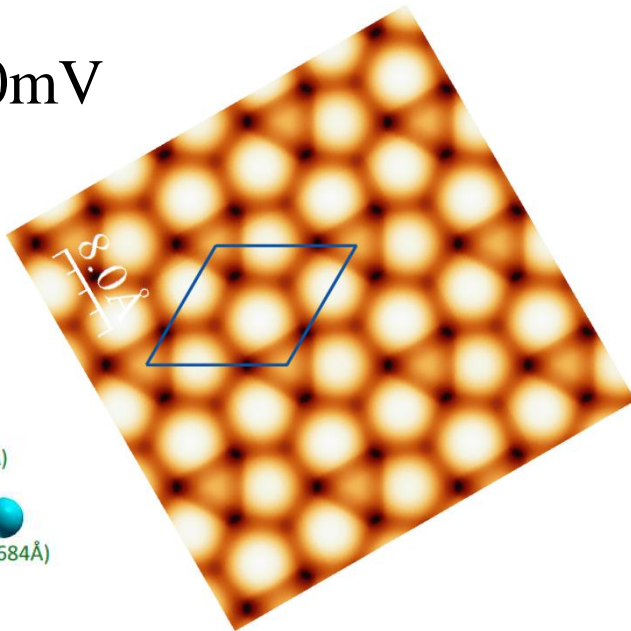
$V=100\text{mV}$



The calculations were performed by the Tersoff-Hamman approximation, and an isovalue of $8 \times 10^{-7} \text{ e/bohr}^3$ was used for generation of the height profile for both the cases.

Regularly buckled

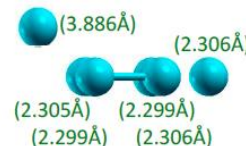
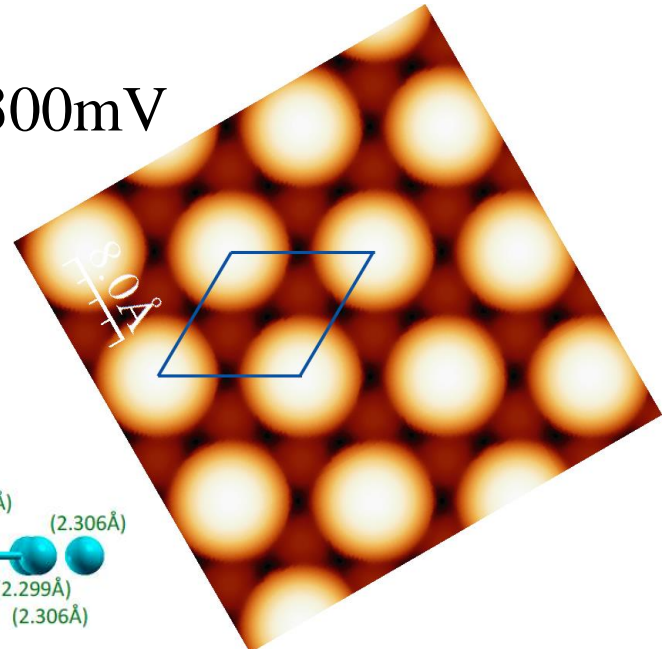
$V=+300\text{mV}$



Si_B is blight.

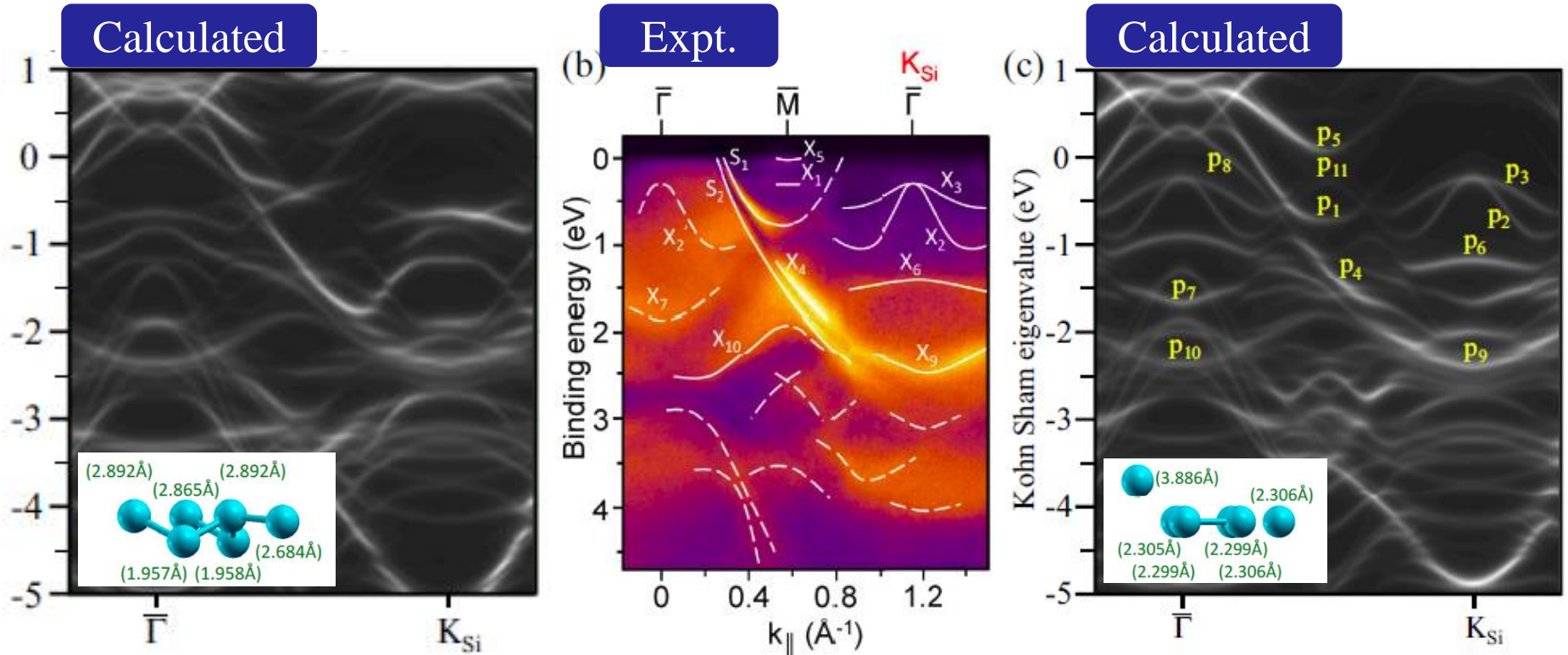
Planar-like

$V=+300\text{mV}$



Si_C is blight.

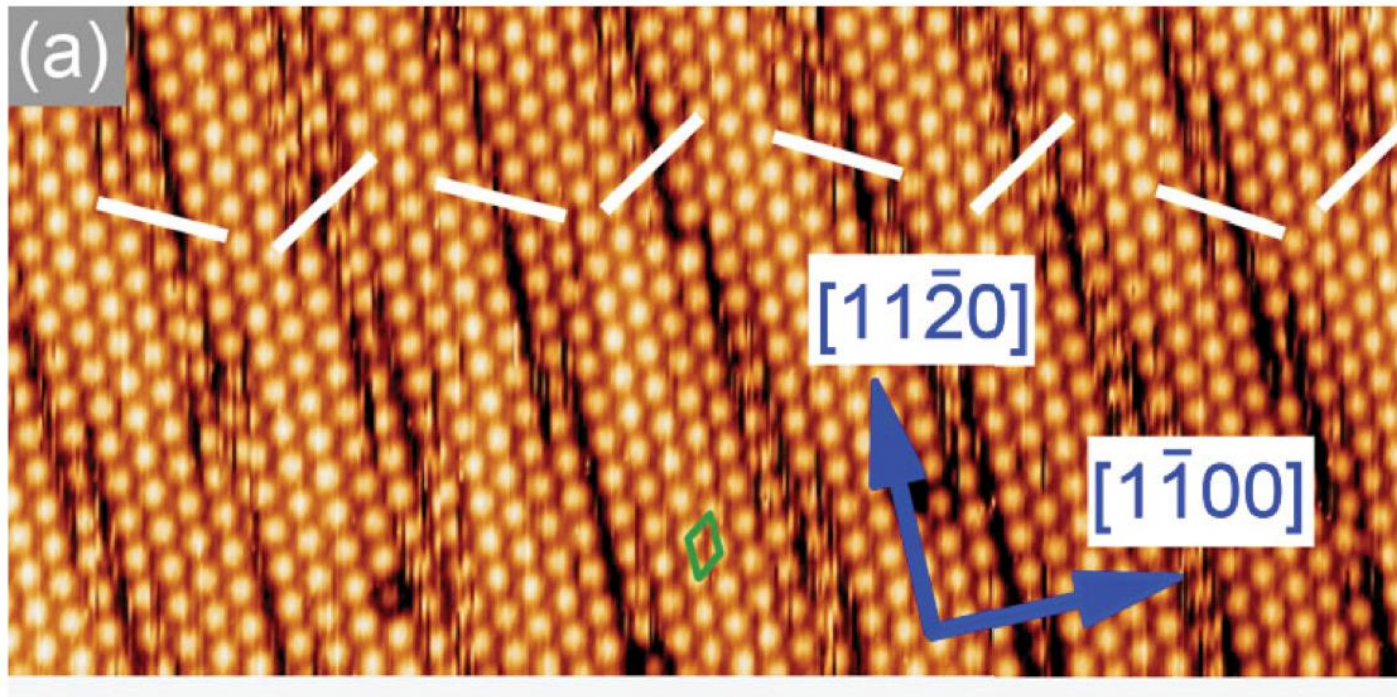
ARPES and calculated bands



The ARPES intensity spectrum is well reproduced by the band structure of planar-like structure more than that of the buckled like structure, especially for S_1 , S_2 , X_2 and X_3 bands.

Domain structure of silicene on ZrB_2

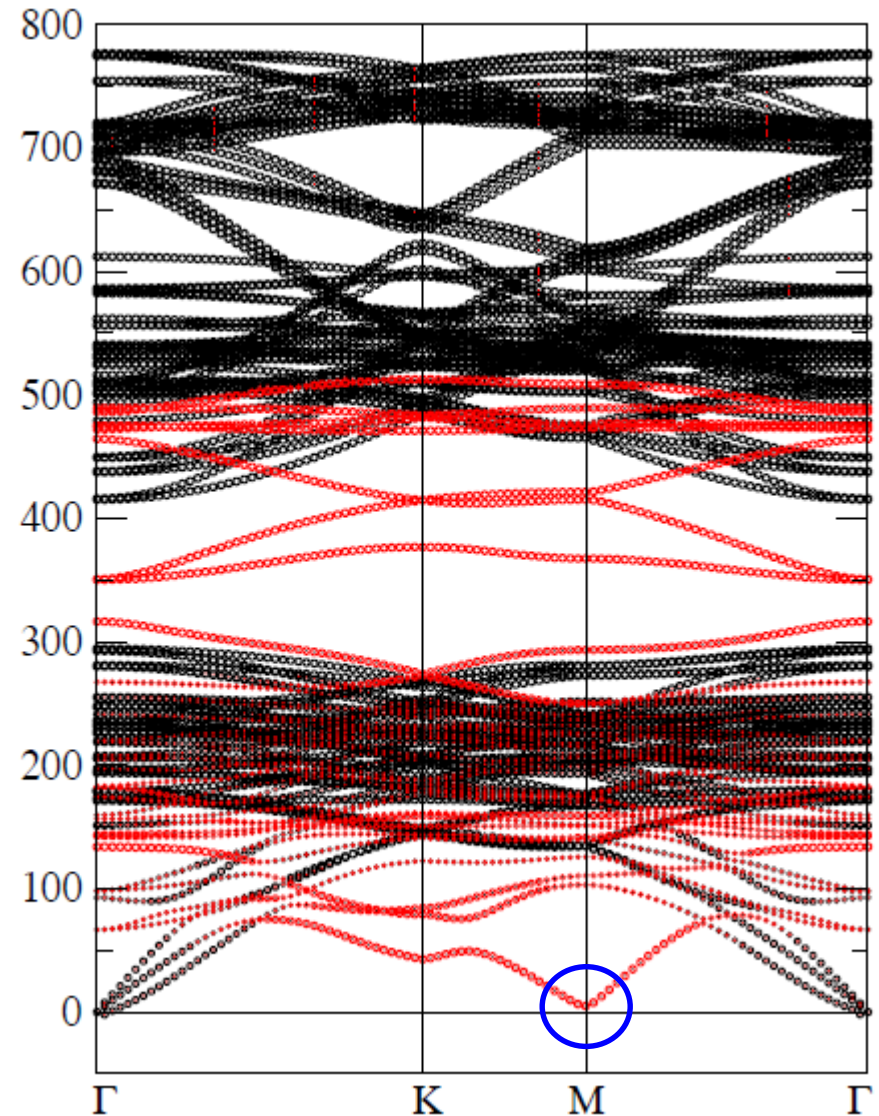
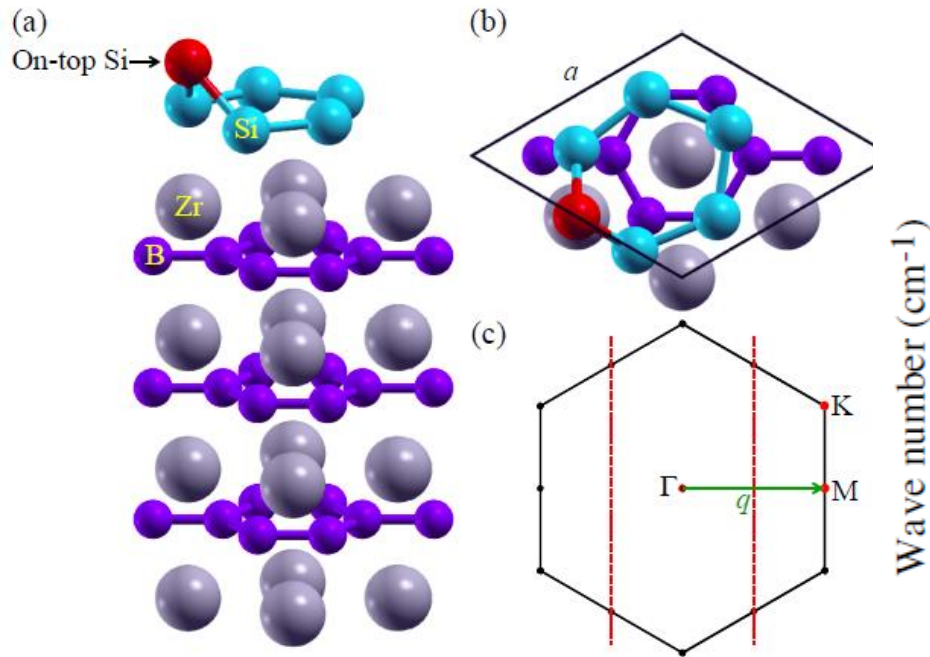
- Silicene on ZrB_2 spontaneously forms a domain (stripe) structure.
- Release of strain might be a reason for that to reduce the areal density of Si.



A. Fleurence et al., PRL 108, 245501 (2012).

Phonon dispersion of silicene on ZrB_2

C.-C. Lee et al., Phys. Rev. B 90, 241402 (2014).

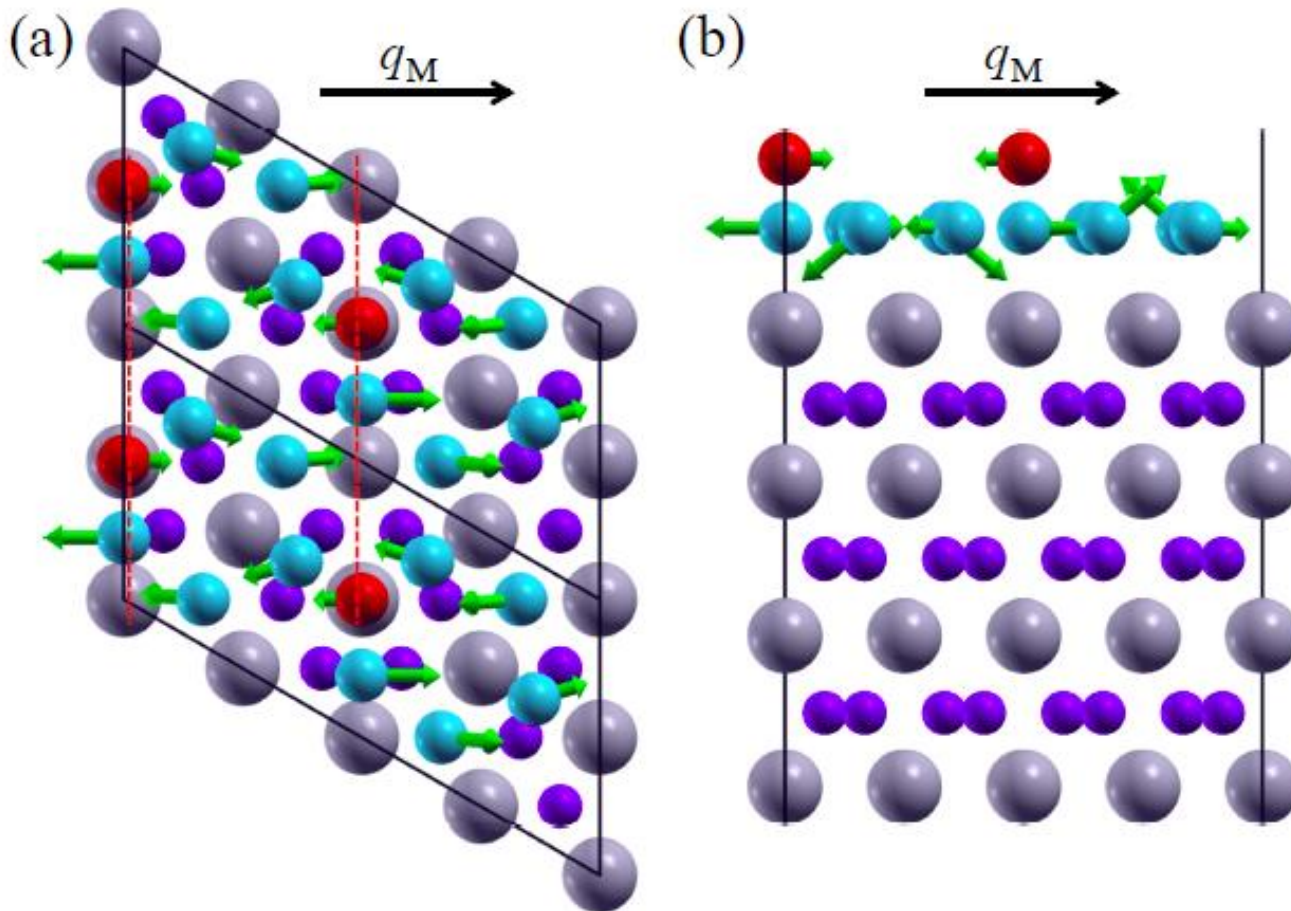


The softest mode reaches the “zero” frequency at the M point.

red: silicene black: ZrB_2

Eigendisplacement at the M-point with zero frequency

All the Si atoms move nearly perpendicular to the red dot line formed by connecting the top Si atoms.



Avoiding the six M-points with zero frequency

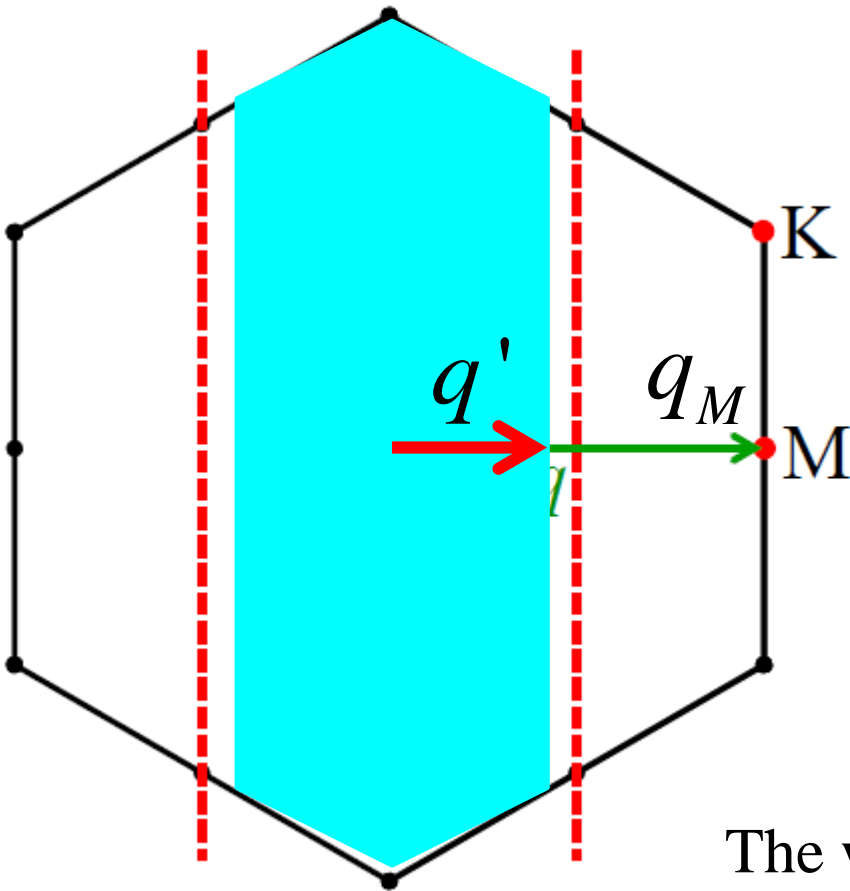
The six M-points can be avoided by changing the BZ as shown below.

Condition

$$q' < \frac{q_M}{2}$$

$$q' \times \frac{\sqrt{3}}{2} a \times N = 2\pi \quad \downarrow \quad q_M = \frac{2\pi}{\sqrt{3}}$$

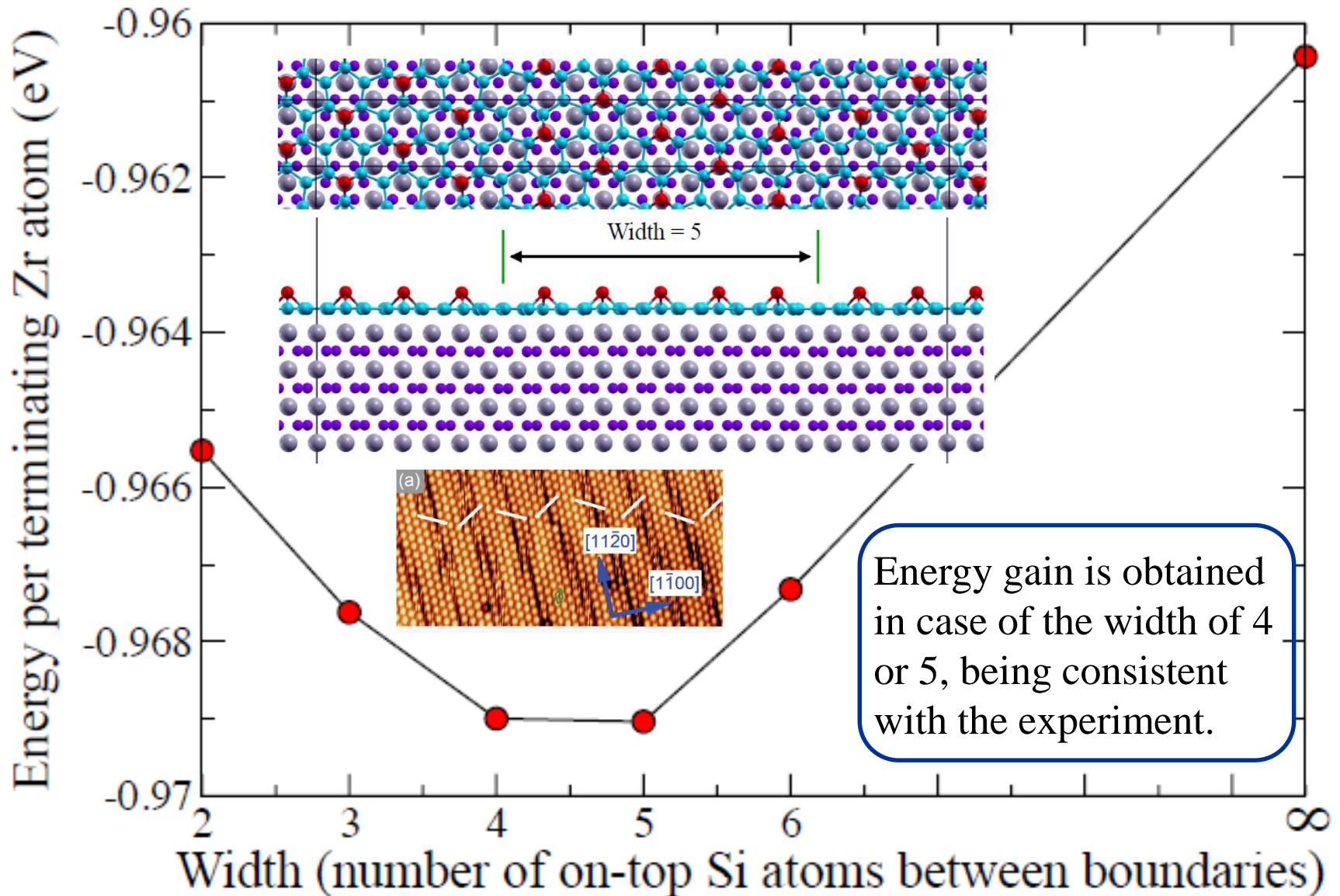
$$4 < N$$



The width N should be larger than 4 to avoid the six M-points.

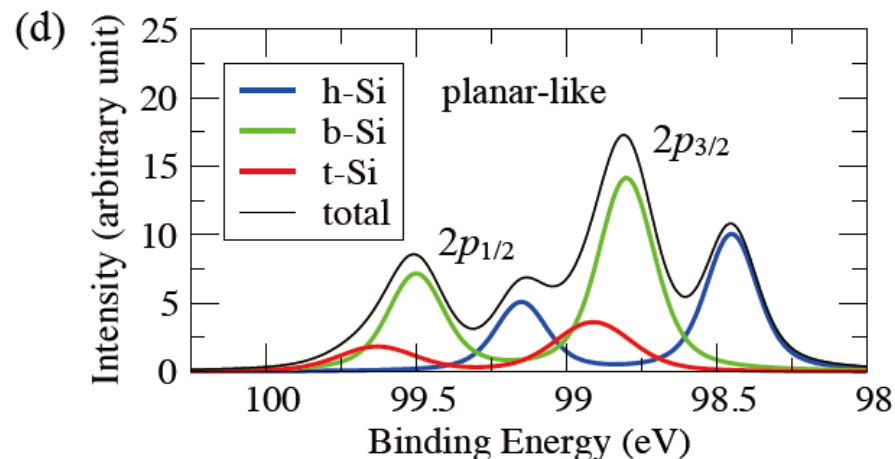
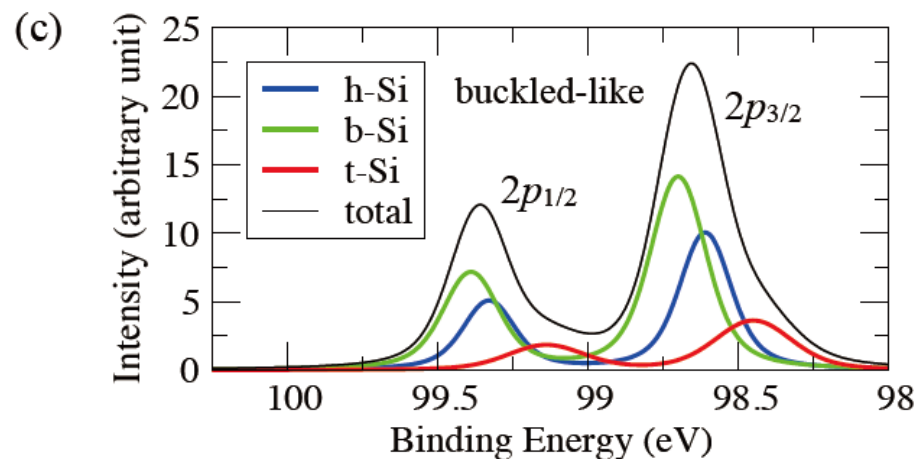
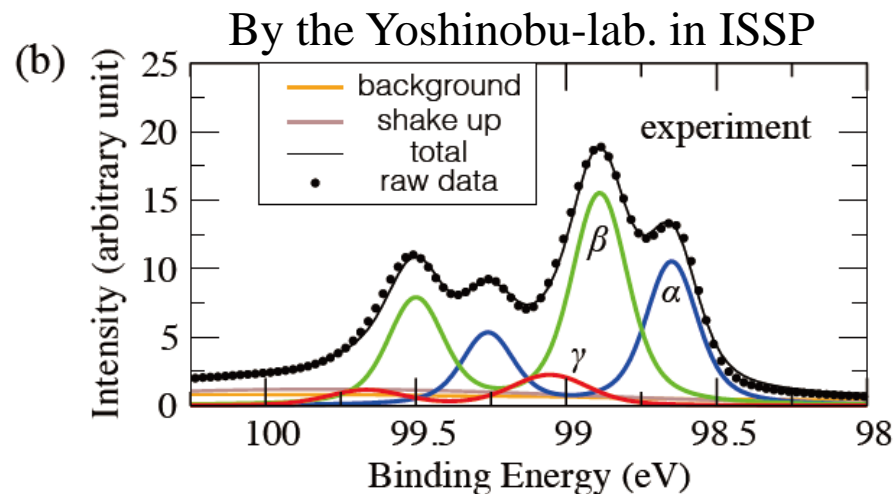
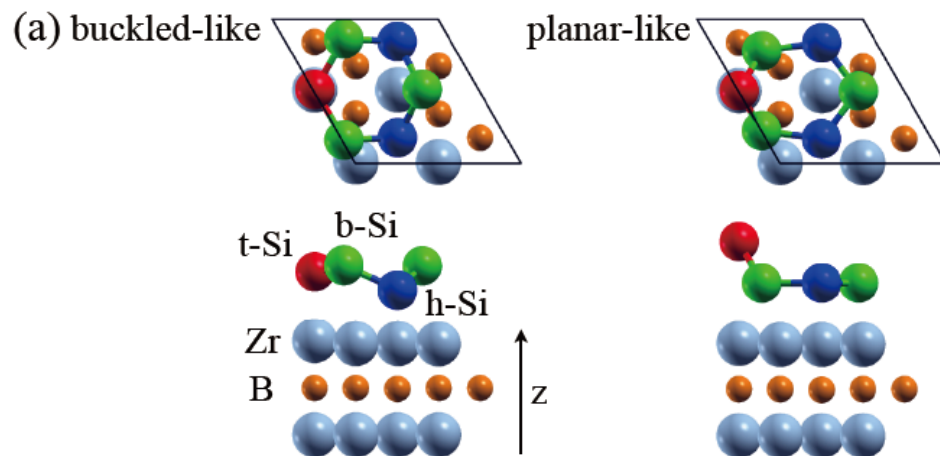
Total energy calculations of the domain structures

C.-C. Lee et al., Phys. Rev. B 90, 241402 (2014).



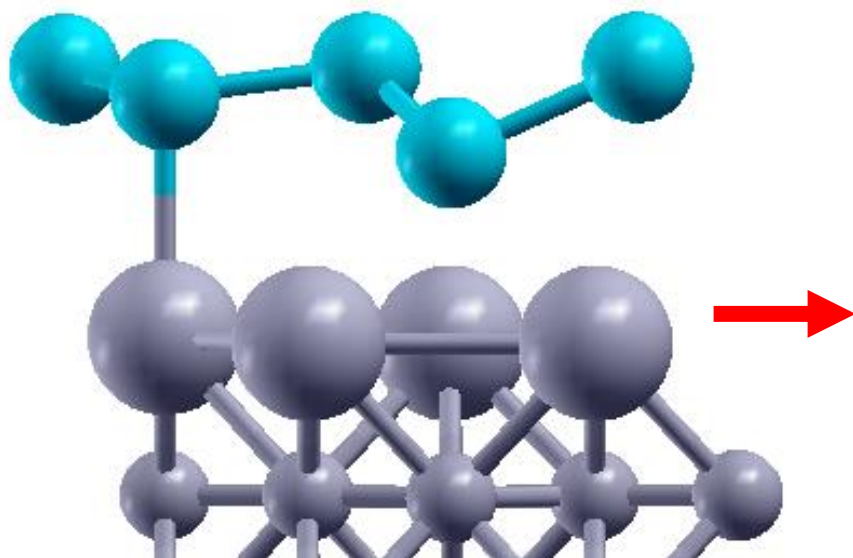
XPS of Si-2p: Expt. vs. calculations

The XPS data is well compared with the calculated binding energy of planar-like structure.

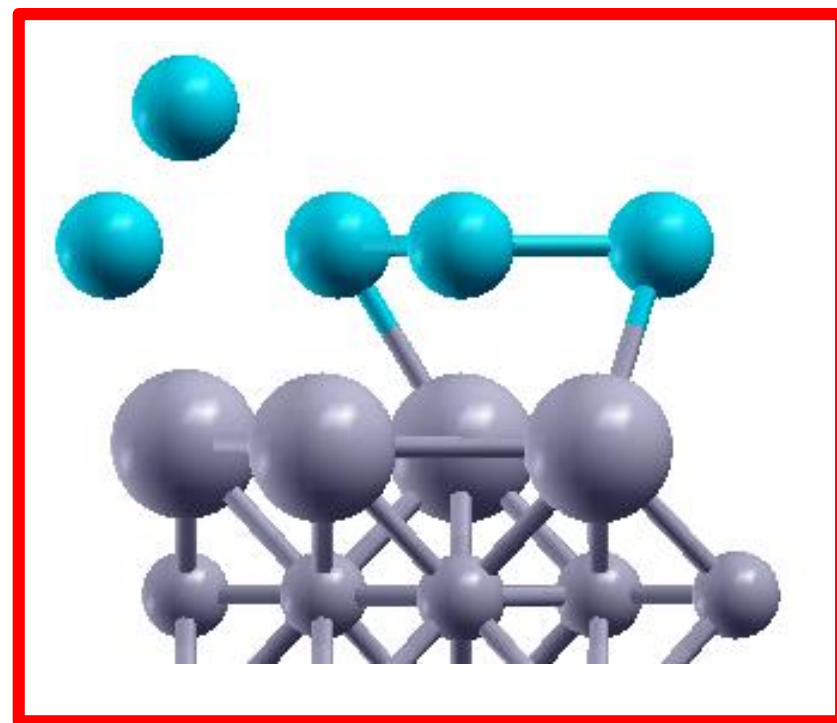


Characterization of structure by expt. and calcs.

In 2012, a regularly-buckled structure was supposed.



The DFT calculations of ARPES, phonon, and XPS strongly support a planar structure. Our collaborators also agree our conclusion.



Summary

We have developed a novel method to calculate absolute binding energies of core levels for solids with the following features:

- applicable to **insulators** and metals
- accessible to **absolute** binding energies
- screening of core and valence electrons on the same footing
- SCF treatment of spin-orbit coupling
- exchange interaction between core and valence states
- geometry optimization with a core hole state

By applying the method for silicene on ZrB_2 , we have obtained a conclusive agreement between the experiments and calculations.

TO and C.-C. Lee, Phys. Rev. Lett. 118, 026401 (2017).

C.-C. Lee et al., Phys. Rev. B 95, 115437 (2017).